CFD Simulations of a Supersonic Ejector for Use in Refrigeration Applications

David SCOTT*, Zine AIDOUN, Omar BELLACHE and Mohamed OUZZANE

Natural Resources Canada, CETC-Varennes
Varennes, Québec, Canada
(tel: 450-652-4481, fax: 514-652-5177, david.scott@nrcan.gc.ca)

ABSTRACT

Supersonic ejectors have been used in cooling/refrigeration applications since the early 1900s. Interest in supersonic ejectors has been rekindled by recent efforts to reduce energy consumption; ejector refrigeration systems can be powered by solar energy or by waste heat generated by another process. This paper presents the results of computational fluid dynamics (CFD) simulations of a supersonic ejector for use in a refrigeration system. The proposed model was applied to a geometry corresponding to an experimental apparatus that operates using R245fa. The impact of varying operating conditions (generator and evaporator pressures) on the ejector entrainment ratio and critical condenser pressures was investigated. Other parameters considered in this study include: the primary nozzle exit position; the length of the mixing chamber; and the diameter of the secondary flow inlet. The results show that CFD is a useful tool in the design of ejectors for refrigeration applications.

1. INTRODUCTION

Ejectors have long been used in cooling applications and as vacuum generators. They have not been favoured for use in refrigeration systems due to the relatively low Coefficient of Performance (COP) of ejector refrigeration systems in comparison with vapour-compression or absorption refrigeration systems. However, their simple mode of function, lack of moving parts and capability of driving a refrigeration device primarily through the use of waste heat or solar energy make them particularly attractive in this energy-conscious era. In addition, using waste heat or solar energy to power a refrigeration system will reduce the electrical energy consumption used to power vapour-compression refrigeration systems, potentially reducing the emissions of greenhouse gasses that are associated with the production of electricity from fossil fuel burning power plants. The purpose of this paper is to present the results of CFD (Computational Fluid Dynamics) simulations of a supersonic ejector for use in a refrigeration system. This numerical model can be used as a design tool to improve the operation of ejectors, specifically by investigating the impact of various operating conditions and geometrical factors on the ejector entrainment and compression ratios.

Many previous numerical models of ejectors have been limited to one-dimensional analyses. In order to better understand the function of ejector refrigeration systems, a commercially available CFD code has been used to create and solve a two-dimensional, axi-symmetric model of a supersonic ejector. The CFD code uses the Finite Volume Method (FVM) to solve the coupled partial differential equations of fluid flow. The present numerical model has been validated by comparing the results to those of Huang et al. (1999), Rusly et al. (2005) and Ablwaifa (2006). These studies include experimental investigations, one-dimensional and two-dimensional, axi-symmetric CFD models of ejectors. The goals of this article are: to compare the results of the present model with those from studies that used the refrigerants R141b and R245fa; to use the model to simulate a new ejector geometry; and to conduct a preliminary parametric study that will help identify key features that may impact ejector performance.

1.1 Ejector refrigeration cycle

The simplest form of a refrigeration cycle (the Carnot cycle) consists of a refrigerant cycling through four components. First, the refrigerant flows through an evaporator where it absorbs energy and changes phase from liquid to vapour. Second, a compressor is used to increase the pressure of the refrigerant. Third, a condenser is used to reject heat from the refrigerant. Fourth, an expansion device is used to decrease the pressure of the refrigerant to the pressure desired in the evaporator where the cycle begins again. In most modern refrigeration systems, a mechanical compressor is used as the second component of the Carnot cycle. Supersonic ejectors can provide an alternative method of providing the required compression. Where conventional vapour compression systems

generally use electrically powered mechanical compressors, thermal energy from existing processes can be recovered to drive the ejector. A schematic illustration of an ejector refrigeration system is shown in Fig. 1.

As illustrated in Fig. 1, ejectors generally consist of a primary fluid that flows through a converging-diverging nozzle, exhausts into a chamber in which there are secondary inlets and a single outlet. In regular operation, the primary fluid is vapourized in the generator and accelerated to supersonic velocities in the converging-diverging nozzle. The supersonic primary flow exits the nozzle at low pressure and entrains a secondary flow of vapour from the evaporator. The two streams mix, and a series of shock waves result that reduce the flow to sub-sonic velocities. The combination of the shock waves and of the sub-sonic flow through the diffuser increase the pressure of the flow to that found at the condenser.

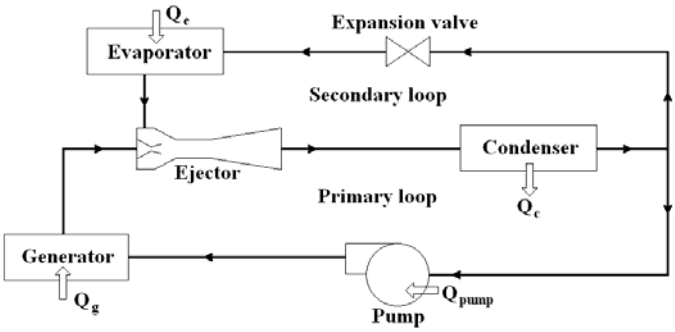

Figure 1: A basic ejector refrigeration cycle.

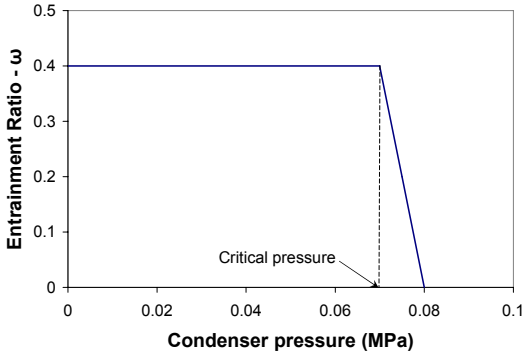

Figure 2: Ejector characteristics.

Summaries of the studies on the use of ejectors in cooling and refrigeration applications are available in the review papers of Sun and Eames (1995) and Chunnanond and Aphornratana (2004). These review papers cover the development of ejector flow theory and the advances in one-dimensional modeling of ejectors, thus a comprehensive review of these topics will not be given here.

Only recently has Computational Fluid Dynamics (CFD) been used to investigate the performance of ejectors in refrigeration applications. CFD simulations have an advantage in that they do not require the input of any nozzle efficiencies or other 'correction factors' that are often used in one-dimensional models. Thus, previous knowledge of empirical results is not required in order to accurately model the performance of the ejector. Riffat et al. (1996) were among the first to publish results of CFD simulations of ejectors for use in refrigeration applications. They simulated ejectors operating with three different refrigerants, ammonia, R134a and propane. The fluids were assumed to be incompressible in their analysis. Riffat and Omer (2001) extended this work to include compressibility effects in the analysis of a methanol ejector. The results compared well with those from complementary experimental tests. The influence of different turbulence models on the results of CFD models of air ejectors has been studied by Bartosiewicz et al. (2005). Further to this, Bartosiewicz et al. (2006) performed CFD studies of ejectors that use the real properties of R142b rather than an idealized model (such as the perfect gas model) in the description of the thermophysical properties of the refrigerant. Eames and Ablwaifa (2004) performed CFD simulations of steam ejectors using constant fluid properties except for the density which was treated using the ideal gas model. In further work, Ablwaifa (2006) continued with CFD simulations of several different ejector designs, as well as using refrigerants R236fa and R245fa. The results of these simulations were compared to the results of complementary experimental tests. CFD simulations of ejectors operating using R141b were performed by Rusly et al. (2005). Their results were compared well to the experimental results of Huang et al. (1999), as well as to the results of a one-dimensional model of Huang's ejectors.

1.2 Ejector theory

An important characteristic of an ejector is the entrainment ratio ω, or the ratio of the mass flow rate of the entrained secondary fluid to that of the primary fluid. A key feature of supersonic ejectors is the constant entrainment ratio that exists under certain operating conditions. The constant capacity behavior of an ejector is observed when, for fixed generator and evaporator pressures, the entrainment ratio of the ejector remains constant with increases in condenser pressure until a critical condenser pressure (p_c*) is reached. Once the critical condenser pressure is reached, the entrainment ratio rapidly drops and the ejector ceases to function. An example of this can be seen in

Fig. 2. Munday and Bagster (1977) proposed that the constant capacity of an ejector is caused by choking of the secondary fluid before it mixes with the primary fluid. Since both the primary and secondary flows are choked, the entrainment ratio will remain constant until the condenser pressure increases to a point that the secondary flow is no longer choked.

2. MODELING OF THE PROBLEM

A general schematic drawing of the ejectors used in the numerical simulations is shown in Fig. 3. It is assumed that the ejectors are axi-symmetric, thus only the top half of the drawn ejector will be modeled in this work; there is a line of symmetry on the z-axis.

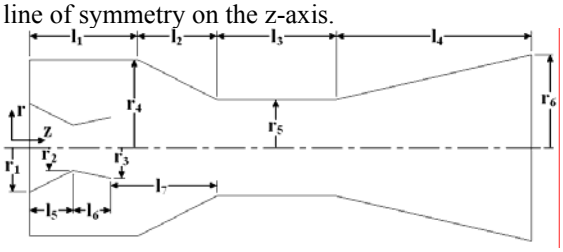

Figure 3: Ejector geometry

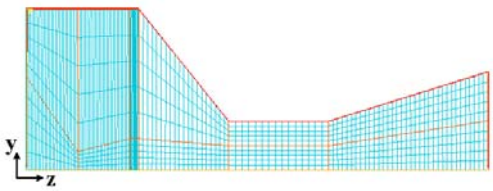

Figure 4: Sample of the base grid used in the domain discretization (not to scale).

2.1. Governing equations

The ejectors modeled in this study are considered to be two-dimensional, axi-symmetric with steady-state flows of compressible fluids. The commercial CFD code PHOENICS V3.5.1 was used for the simulations. Under steady-state conditions, derivatives with respect to time can be neglected and the governing equations can be expressed in the following general form:

$$\frac{\partial}{\partial x_k}\left(\rho \boldsymbol{U}\varphi - \Gamma_\varphi \frac{\partial \varphi}{\partial x_k}\right) = S_\varphi \qquad (1)$$

Specific definitions of the variables φ, Γ_φ and S_φ for the cases of the continuity, momentum and energy equations are provided in Table 1.

Table 1: Values of φ, Γ_φ and S_φ in Eq. 1.

Variable	φ	Γ_φ	S_φ
Continuity	1	0	0
z-momentum	w	$\rho(\nu_t+\nu_L)$	$-\frac{\partial p}{\partial z} + gravity + friction...$
r-momentum	v	$\rho(\nu_t+\nu_L)$	$-\frac{\partial p}{\partial r} + gravity + friction...$
Energy	h	$\rho\left(\frac{\nu_t}{\mathrm{Pr}_t} + \frac{\nu_L}{\mathrm{Pr}\,L}\right)$	$-\frac{Dp}{Dt} + heat\ sources + ...$

The effects of turbulence in the ejector have been accounted for through the use of the standard k-epsilon turbulence model of Launder and Spalding (1972). While CHAM (2003) notes that this model is not always recommended for simulations of compressible flows or of jet flows, Ablwaifa (2006) found that simulations using this turbulence model yielded good results for the simulation of fluid flow in ejectors using R141b as the working fluid.

2.2. Calculation Procedure

A body-fitted-coordinates (BFC) grid was used in the calculations. A base grid consisting of 10 volumes in the r-direction and 113 volumes in the z-direction, shown in Fig. 4, was used for initial calculations. The grid was further refined by increasing the grid density by a grid refinement factor (δ = 1, 2, 3, 4). The CFD results from the runs with different grid densities were then compared both qualitatively and quantitatively in order to determine the dependence of the grid on the results. It was found that the results were essentially independent of grid when a refinement factor of δ= 4 was used.

A staggered grid formulation has been used in the solution; scalar quantities (pressure, enthalpy, thermophysical properties) are stored at nodes at the centre of the control-volumes, and vector quantities (velocities) are stored at points at the centre of the control volume faces. The SIMPLEST procedure of Spalding (1980) was used to solve the nonlinear coupled sets of discretized equations for v, w, P and H. The discretization of the transport terms related to the convection and diffusion fluxes have been treated using the hybrid scheme of Patankar (1980).

2.3. Geometry and Boundary Conditions

The geometry of the CFD model was initially set to simulate the AB and AG geometries of Huang et al. (1999). The temperatures at the primary and secondary inlets were also taken directly from Huang et al.; the pressures at inlets were taken as the corresponding saturation pressures. An outlet pressure of 0.06 MPa was used to determine the grid-independent entrainment ratio. A summary of the geometry, using Fig. 3 as a reference, is given in Table 2. In the model, the no-slip boundary condition was used on all solid surfaces. The z-axis was an axis of symmetry. The operating conditions, reference results and results of the CFD model are summarized in Table 3.

Table 2: Geometry from Huang et al. (1999) used in the validation of the CFD model.

	Lengths (mm)							Radii (mm)					
	l_1	l_2	l_3	l_4	l_5	l_6	l_7	r_1	r_2	r_3	r_4	r_5	r_6
AB	40	32.24	35.6	56.94	18.32	18.32	35.6	6.65	1.32	2.25	11.55	3.49	7.04
AG	40	32.24	35.6	56.94	18.32	18.32	35.6	6.65	1.32	2.25	11.55	3.67	7.04

Table 3: Summary of ejector operating conditions

Model	P_g [MPa]	T_g [^{o}C]	P_e [MPa]	T_e [^{o}C]	E.R. CFD	E.R. Exp[1]	E.R. 1D[1]	E.R. CFD[2]
AB1	0.4006	78	0.03999	8	0.3982	0.3922	0.4422	0.4097
AB2	0.4655	84	0.03999	8	0.3266	0.3117	0.3042	0.337
AB3	0.5380	90	0.03999	8	0.2673	0.2718	0.2093	0.2749
AG1	0.4006	78	0.03999	8	0.4712	0.4393	0.4609	0.4395
AG2	0.4655	84	0.03999	8	0.3986	0.3883	0.3704	0.3977
AG3	0.5380	90	0.03999	8	0.3319	0.304	0.2395	0.3343
AG4	0.6046	95	0.03999	8	0.2821	0.2552	0.2144	0.248
AG5	0.4006	78	0.04728	12	0.5834	0.6132	0.6659	0.5775
AG6	0.4655	84	0.04728	12	0.4893	0.479	0.4769	0.4835
AG7	0.5380	90	0.04728	12	0.4093	0.4034	0.4142	0.3831
AG8	0.6046	95	0.04728	12	0.3505	0.3503	0.3434	0.3548

[1] Results from Huang et al. (1999). [2] Results from Rusly et al. (2005)

The working fluid for the model was R141b. The thermophysical properties of R141b were calculated with the use of the NIST REFPROP v7.0 database (2002). The thermal conductivity, specific heat and viscosity were considered to be constant throughout the calculation domain. The value of these properties was taken as an averaged value of those calculated using REFPROP at each node in the domain. REFPROP was also used to determine the variation of the density of R141b in the superheated region; a correlation equation was used that curve-fit the variation of density with both pressure and enthalpy.

2.4. Validation using models with R141b

The entrainment ratio of the ejector is determined by calculating the ratio of the mass flow rate of refrigerant through the generator to the mass flow rate of refrigerant from the evaporator. As discussed previously, the entrainment ratio remains essentially constant for condenser pressures below a critical value. Above the critical condenser pressure, the mass flow rate from the evaporator rapidly decreases.

A comparison of the experimentally measured and numerically calculated entrainment ratios for all ejector models and geometries used in this study is shown in Table 3 and in Fig. 5. The results of the proposed model compare well with the experimental results. Also shown in Table 3 and Fig. 5 are the results of the 1D model of Huang et al. (1999) and of the CFD model of Rusly et al. (2005). The solid line represents a perfect correlation of the modeling and experimental results. Results of the models, including the current CFD, 1D of Huang et al. (1999) and CFD of Rusly et al. (2005) are shown as points. Results closer to the solid line indicate a closer comparison. The differences between the experimental and the calculated entrainment ratios are between -4.9% and 10.6%; for the 1-

D analysis of Huang et al., the differences are between -23.0% and 12.8%; and for the CFD results of Rusly et al., the differences range from -5.8% to 10.0%. The proposed CFD model is thus comparable to that of Rusly et al., both of which improve significantly on the 1-D model.

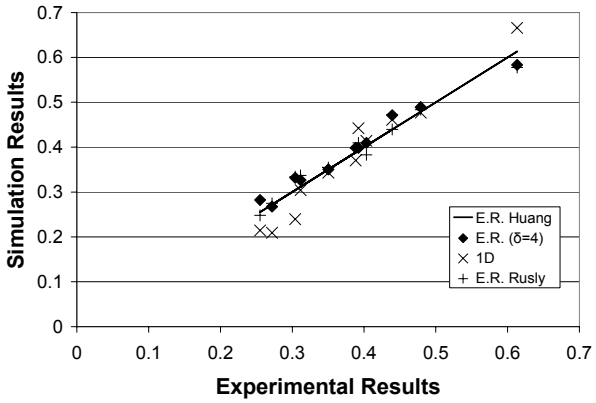

Figure 5: Comparison of the entrainment ratios of Huang et al. (1999) with those from different models.

2.5. Validation using R245fa

Experimental data and CFD results for ejectors operating using R245fa can be found in Ablwaifa (2006). Validation of the present CFD model has been performed using the 'optimized' geometry of Ablwaifa. In the 'optimized' ejector geometry, Ablwaifa (2006) uses two converging sections; the curved section in which the majority of convergence from the evaporator entry diameter to the mixing chamber takes place, and the linear converging section where the remaining convergence occurs (l_2 and l_3 in the above diagram, respectively). The geometry used in the present CFD studies corresponds to the 'optimized' R245fa conventional jet-pump of Ablwaifa.

Table 4: Summary of ejector operating conditions: 'optimized' geometry (β=1.34)

Case	P_g [MPa]	T_g [^{o}C]	P_e [MPa]	T_e [^{o}C]	ω (exp[1])	ω (CFD)	ω (CFD[2])	p_c* [MPa] (exp[1])	p_c* [MPa] (CFD)	p_c* [MPa] (CFD[2])
OPTI1-8	1.261	100	0.07622	8	0.482	0.454	0.5	0.2059	0.2110	0.2130
OPTI1-10	1.261	100	0.08293	10	0.518	0.483	0.55	0.2094	0.2109	0.2167
OPTI1-12	1.261	100	0.09009	12	0.564	0.512	0.58	0.2130	0.2142	0.2204
OPTI1-15	1.261	100	0.1018	15	0.628	0.560	0.63	0.2182	0.2181	0.2241
OPTI2-8	1.407	105	0.07622	8	0.387	0.413	0.42	0.2241	0.2293	0.2318
OPTI3-8	1.565	110	0.07622	8	0.334	0.359	0.35	0.2436	0.2451	0.2559
OPTI4-8	1.736	115	0.07622	8	0.261	0.285	0.29	0.2687	0.2594	0.2820
OPTI5-8	1.921	120	0.07622	8	0.228	0.205	0.27	0.2865	0.2628	0.3005

[1] Experimental and; [2] CFD results of Ablwaifa (2006)

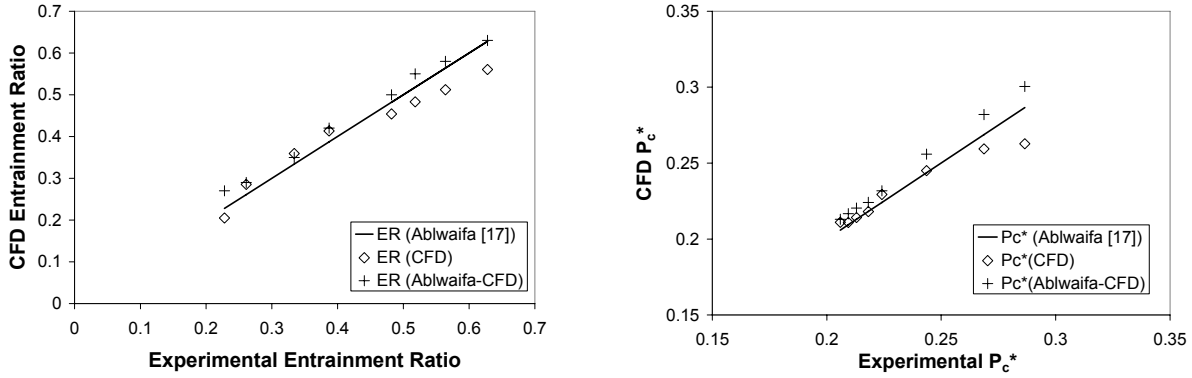

(a) Entrainment ratio (b) Critical condenser pressure

Figure 6: Comparison of the entrainment ratios and the critical condenser pressures (p_c*) determined experimentally and by the CFD model.

The results of the eight cases run for validation of the CFD model are presented in Table 4, along with Ablwaifa's (2006) experimentally determined values of the entrainment ratio and of the calculated critical condenser pressure. The differences between the experimentally determined entrainment ratios and those obtained using the proposed CFD model vary between -10.8% and +9.3%. The differences between the calculated critical condenser pressures vary between -8.3 and 2.5%. This is shown graphically in Figs. 6a and 6b, where a comparison between the CFD calculated and the experimentally measured values are presented for the entrainment ratio and the critical condenser pressure, respectively. It is clear that the results of the proposed CFD model agree well with those of Ablwaifa's CFD model. The results of the proposed CFD model are in good agreement with the corresponding experimental results; the difference between the results of the proposed model and those from experiments is less than 10.8% for the 'optimized' ejector configuration of Ablwaifa over all operating conditions considered.

3. RESULTS AND DISCUSSION

3.1. New geometry with R245fa

The validated CFD model was then applied to a geometry that corresponds to an experimental test bench being built in-house at CETC-Varennes. Key dimensions of this geometry, (refer to the schematic illustration of Fig. 3), are: L_1=27.0mm, L_2=L7=36.0mm, L_3=37.36mm, L_4=85.78mm, L_5=17.0mm, L_6=10.0mm, L_7=L_2, R_1=3.0mm, R_2=1.48mm, R_3=2.35mm, R_4=15.0mm, R_5=4.5mm and R_6=12.14mm. In addition to these dimensions, a 29.79mm long entrance length was added (where R1 and R4 remain constant), as was an adiabatic wall of finite thickness for the primary nozzle (outside radius of 9.525mm with a 45^o bevel 2.0mm from the outside wall). Once the model was applied to this geometry (hereafter referred to as CETC-A), the model was run for a range of operating conditions (shown in Table 5). Also contained in Table 5 are the results of the simulations: the calculated entrainment ratio (ω) and critical condenser pressure (p_c*) for each operating condition. The results are graphically presented in Fig. 7.

Table 5: Summary of CETC-A CFD runs showing entrainment ratio and critical condenser pressure.

	Entrainment ratio [critical condenser pressure (kPa)]			
Evaporator inlet saturation temperature (^{o}C)	Generator inlet saturation temperature (^{o}C) / [saturation pressure (kPa)]			
	60^{o}C [463.52kPa]	80^{o}C [788.81kPa]	100^{o}C [1261.4kPa]	120^{o}C [1920.5kPa]
-10^{o}C	0.232 [75.24]	0.047 [100.3]	Not run	Not run
-5^{o}C	0.333 [83.23]	0.111 [111.8]	Not run	Not run
0^{o}C	0.459 [91.65]	0.194 [123.1]	0.038 [160.3]	Not run
5^{o}C	0.606 [99.56]	0.274 [137.6]	0.092 [177.7]	Not run
10^{o}C	0.780 [109.8]	0.370 [150.1]	0.160 [195.5]	0.030 [244.9]
15^{o}C	0.981 [120.2]	0.488 [162.9]	0.228 [215.0]	0.076 [268.3]
20^{o}C	1.224 [135.0]	0.621 [175.7]	0.306 [234.3]	0.132 [294.6]

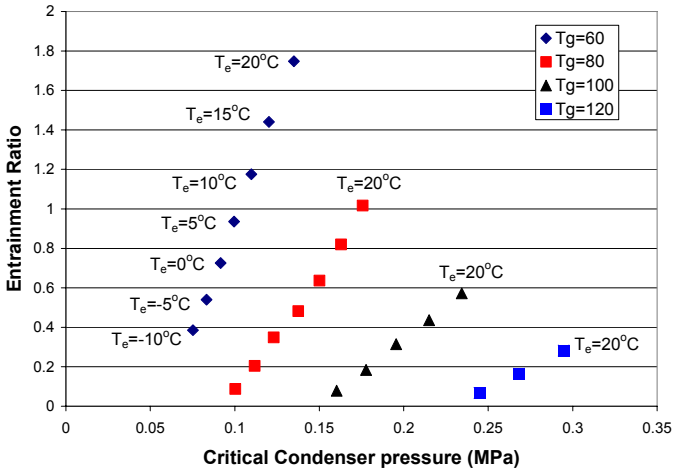

Figure 7: Predicted variation of the entrainment ratio with the critical condenser pressure for the CETC-A ejector.

The data shown in Fig. 7 effectively characterizes the CETC-A ejector. For fixed conditions at the generator, both the entrainment ratio and the critical condenser pressure increase with evaporator temperature. For fixed conditions in the evaporator, increases in the generator temperature result in a decrease in the entrainment ratio and an increase in the critical condenser pressure. These results are typical of single-phase supersonic ejectors.

4. PARAMETRIC ANALYSIS

The CETC-A geometry was used as the base case for a parametric analysis that helped to determine key features of the ejector geometry that impact overall performance. The operating conditions were fixed at T_g=80°C and T_e=10°C. Three specific geometrical parameters were varied in this analysis: the nozzle exit position (NXP); the length of the mixing chamber (LM); and the diameter of the secondary flow (evaporator) inlet (DE). The impact of varying these parameters is shown in Figs. 8a, b and c, respectively.

The data shown in Fig. 8 shows that these three parameters, the nozzle exit position, the mixing length and the evaporator inlet diameter, appear to have little impact on the performance of the ejector. In all of these cases, it is possible to find a performance maximum, however the impact of changes in these parameters is small. Of the three parameters considered, the parameter with the greatest impact on the entrainment ratio is the nozzle exit position; however, the variation of the entrainment ratio is less than 4.1% throughout the range considered. The parameter with the greatest impact on the critical condenser pressure is the mixing length (L_3), however the impact is again not large; the variation between the minimum and maximum calculated values is only 5.8%.

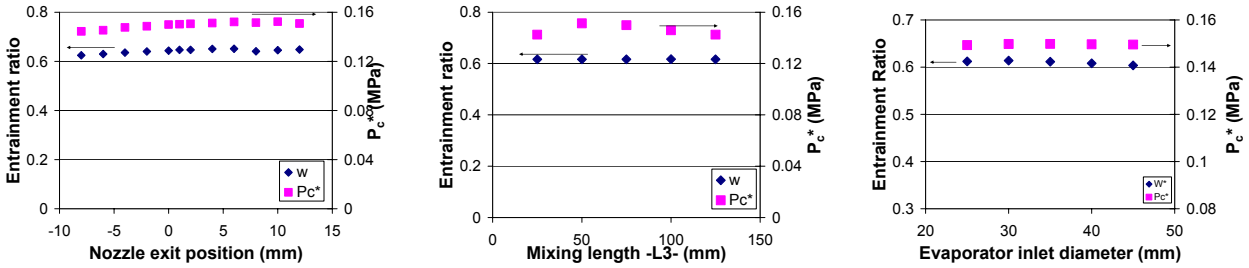

(a) Nozzle exit position (b) Mixing length (c) Evaporator inlet diameter

Figure 8: Results of the geometric parameter analysis on the performance of the CETC-A ejector.

5. CONCLUSIONS

A commercial CFD code was used to create a model of a supersonic ejector. A key feature of the model was the use of the real-gas properties of the refrigerants used. The model was applied to geometries and operating conditions that for experimental investigations that are available in the literature that used R141b and R245fa as the refrigerant. The results from the proposed CFD model are in good agreement with the corresponding experimental results; the maximum difference between the results of the proposed model and the experimental results over all conditions considered was 10.8%.

The validated CFD model was then used to predict the performance of an in-house experimental ejector (CETC-A) over a range of operating conditions.

The CFD model was used to investigate the impact of three geometric parameters on the performance of the CETC-A ejector. Optimum configurations of the nozzle exit position, the mixing length and the evaporator inlet diameter can be identified, however the impact on overall ejector performance is small.

This study shows that CFD is a useful tool for analyzing and designing supersonic ejectors.

NOMENCLATURE

A	constant used to determine ξ_{GI}	
h	enthalpy	(kJ/kg)
l	lengths of the ejector in the z-direction	(m)
m	constant used to determine ξ_{GI}	
p	pressure	(kPa)
Pr	Prandtl number	
Q	Rate of heat transfer	(W)
r	radial direction	(m)
S_φ	source term for φ	
T	temperature	(^oC)
U	velocity vector	(m/s)
v	radial direction velocity vector	(m/s)
w	axial direction velocity vector	(m/s)
z	axial direction	(m)

Greek Symbols

δ	grid refinement factor	
φ	variable to be solved	
ξ	generic result of interest	
ρ	density	(kg/m^3)
ν	kinematic viscosity	(m^2/s)
Γ	diffusion coefficient for φ	
ω	entrainment ratio	

Subscripts

c	condenser
c*	critical point
e	evaporator
g	generator
GI	grid independent
L	laminar
t	turbulent

REFERENCES

Ablwaifa, A.E., 2006, "Study of a Jet-Pump Used in a Refrigeration System," Ph.D. Thesis, Nottingham U., UK.

Bartosiewicz, Y., Aidoun, Z., Desevaux, P. and Mercadier, Y., 2005, "Numerical and Experimental Investigations on Supersonic Ejectors," Int. J. Heat and Fluid Flow, 26, pp. 56-70.

Bartosiewicz, Y., Aidoun, Z. and Mercadier, Y., 2006, Numerical Assessment of Ejector Operation for Refrigerant Applications Based on CFD," Applied Thermal Engineering, 26, pp. 604-612.

CHAM Ltd., 2003, PHOENICS V3.5.1, Wimbledon, UK.

Chunnanond, K. and Aphornratana, S., 2004, "Ejectors: Applications in Refrigeration Technology," Renewable and Sustainable Energy Reviews, 8, pp. 129-155.

Eames, I.W. and Ablwaifa, A.E., 2004, "Use of CFD in the Prediction of a Jet-Pump Performance," Proc. HPC 2004, 3rd Intl. Conf. on Heat Powered Cycles, October 10-13, Larnaca, Cyprus.

Huang, B.J., Chang, J.M., Wang, C.P. and Petrenko, V.A., 1999, "A 1-D Analysis of Ejector Performance," Int. J. Refrigeration, 22, pp. 354-364.

Launder, B. and Spalding, D., 1972, "Lectures in Mathematical Models of Turbulence," Academic Press, London, England.

Munday, J.T. and Bagster, D.F., 1977, "A New Ejector Theory Applied to Steam Jet Refrigeration," Industrial Engineering Chemistry, Process Design and Development, 16(4), pp. 442-449.

NIST Standard Reference Database 23, "NIST Thermodynamics and Transport Properties of Refrigerants and Refrigerant Mixtures, REFPROP V7.0," 2003.

Patankar, S.V., 1980, "Numerical Heat Transfer and Fluid Flow", Hemisphere Publishing Corp., Washington, DC.

Riffat, S.B., Gan, G. and Smith, S., 1996, "Computational Fluid Dynamics Applied to Ejector Heat Pumps," Applied Thermal Engineering, 16(4), pp. 291-297.

Riffat, S.B. and Omer, S.A., 2001, "CFD Modelling and Experimental Investigation of an Ejector Refrigeration System using Methanol as the Working Fluid," Int. J. of Energy Research, 25, pp. 115-128.

Rusly, E., Aye, L., Charters, W.W.S. and Ooi, A., 2005, "CFD Analysis of Ejector in a Combined Ejector Cooling System," Int. J. Refrigeration, 28, pp. 1092-1101.

Spalding, D.B., 1980, "Mathematical Modelling of Fluid Mechanics, Heat Transfer and mass Transfer Processes", Mechanical Engineering Department Report HTS/80/1, Imperial College of Science, Technology and Medicine, London, UK.

Sun, D-W. and Eames, I.W., 1995, "Recent Developments in the Design Theories and Applications of Ejectors – a Review," J. of the Institute of Energy, 68, pp. 65-79.

ACKNOWLEDGEMENTS

Financial support for this work was provided by the Canadian Federal Government's Program on Energy Research and Development (PERD) and through a fellowship for the first author from the Natural Sciences and Engineering Research Council of Canada. The authors would also like to acknowledge the support of the members of the Refrigeration Group and the supporting staff at Natural Resources Canada, CETC – Varennes.